Journal of Cosmology and
Astroparticle Physics

ERRATUM

Addendum: Cosmological dependence of non-resonantly produced sterile neutrinos

To cite this article: Graciela B. Gelmini *et al* JCAP10(2020)A01

Journal of Cosmology and Astroparticle Physics
An IOP and SISSA journal

Addendum: Cosmological dependence of non-resonantly produced sterile neutrinos

Graciela B. Gelmini, Philip Lu and Volodymyr Takhistov

Department of Physics and Astronomy, UCLA,
475 Portola Plaza, Los Angeles, CA 90095, U.S.A.

E-mail: gelmini@physics.ucla.edu, philiplu11@gmail.com, vtakhist@physics.ucla.edu

Received June 29, 2020
Revised August 26, 2020
Accepted August 26, 2020
Published October 1, 2020

Addendum to: JCAP12(2019)047

Abstract. In this addendum to the article *JCAP* **12** (2019) 047 (arXiv:1909.13328) on the cosmological dependence of non-resonantly produced sterile neutrinos we discuss, using an analytic treatment, the parameter regions of large active-sterile neutrino mixing angles where sterile neutrinos can approach thermalization. We show that these additional considerations affect only large active-sterile neutrino mixing already rejected by different limits. Hence, the allowed sterile neutrino parameter regions are unaffected.

Keywords: cosmological neutrinos, neutrino theory, particle physics - cosmology connection, physics of the early universe

ArXiv ePrint: 1909.13328

https://doi.org/10.1088/1475-7516/2020/10/A01

JCAP10(2020)A01

Contents

1 Introduction

In ref. [1] (from here on Paper I), as well as in its prior abbreviated companion paper [2], we have considered the cosmological dependence of non-resonantly produced sterile neutrinos. We discussed there the sensitivity of sterile neutrino production to cosmologies that differ from the standard radiation dominated cosmology (STD) before Big Bang Nucleosynthesis (BBN), specifically before the temperature of the Universe was 5 MeV. The lower limit on the highest temperature of the radiation-dominated epoch in which BBN happened is close to 5 Mev [3–9]. Thus, the cosmological evolution in the Universe before the temperature of the Universe was about 5 MeV is unknown and could differ from the STD. Alternative cosmologies can often appear in motivated theories. As examples, we have considered two distinct Scalar-Tensor models (ST1 [10] and ST2 [11]), Kination (K) [12–16] as well as Low Reheating Temperature (LRT) scenario [17] (see also e.g. [3–5, 18–22]), besides the STD cosmology (see Paper I for a detailed description of the different models). We discussed how the resulting limits and regions of interest in the mass-mixing $(m_s, \sin^2 2\theta)$ plane are affected for a sterile neutrino of mass m_s that is assumed to have a mixing $\sin\theta$ only with the active electron neutrino.

In Paper I we presented a simplified treatment of sterile neutrino production for the parameter region where mixing angles are very large. There, the momentum $\vec{p}$ distribution $f_{\nu_s}(E,T)$ of sterile neutrinos of energy $E = |\vec{p}|$, which are relativistic at the production temperature T, is not much smaller than the distribution of active neutrinos $f_{\nu_\alpha}(E,T)$. In part of this region sterile neutrinos can thermalize in the Early Universe, so that $f_{\nu_s}(E,T) = f_{\nu_\alpha}(E,T)$. When thermalized, sterile neutrinos have the same number density of one active neutrino species, i.e. during BBN and later $\Delta N_{\rm eff} = 1$ (or close to 1, depending on entropy dilution), a value that is forbidden by present cosmological limits. While neutrino thermalization has been extensively studied with numerical methods (e.g. [4, 23]), in this addendum we analyze these effects analytically.

We show, always using analytic expressions as in our previous studies, that the regions allowed by all sterile neutrino bounds are not affected by the present considerations.

JCAP10(2020)A01

2 Approaching thermalization

In our analysis of Paper I, we assumed $f_{\nu_s} \ll f_{\nu_\alpha}$ and thus neglected the second term on the right hand side of the Boltzmann equation

$$\left(\frac{\partial f_{\nu_s}(E,T)}{\partial T}\right)_{\epsilon=E/T} = -\frac{\Gamma_s(E,T)}{HT}[f_{\nu_\alpha}(E,T) - f_{\nu_s}(E,T)]\,, \tag{2.1}$$

where $\epsilon = E/T = |\vec{p}|/T$ is the T-scaled dimensionless momentum and the derivative on the left hand side is computed at constant ϵ. Here H is the expansion rate of the Universe, which for $T > T_{\rm tr}$ we parameterize as $H = \eta(T/T_{\rm tr})^\beta H_{\rm STD}$, where $H_{\rm STD} = T^2/M_{\rm Pl}\sqrt{8\pi^3 g_*(T)/90}$ is the expansion for the STD cosmology. For the non-standard cosmologies we consider, the scale factor η and the exponent β values are $\eta = 1$ and $\beta = 1$ for K, $\eta = 7.4 \times 10^5$ and $\beta = -0.8$ for ST1, $\eta = 3.2 \times 10^{-2}$ and $\beta = 0$ for ST2, and they transition to the STD at $T_{\rm tr} = 5\,$MeV (see figure 1 of Paper I). We also consider a LRT model with reheating temperature $T_{\rm RH} = T_{\rm tr}$. $\Gamma_s(E,T)$ in eq. (2.1) is the conversion rate of active to sterile neutrinos,

$$\Gamma = \frac{1}{2}\langle P_m(\nu_\alpha \to \nu_s)\rangle \Gamma_\alpha \simeq \frac{1}{4}\sin^2(2\theta_m) d_\alpha G_F^2 \epsilon T^5\,, \tag{2.2}$$

where $d_\alpha = 1.27$ for ν_e and G_F is the Fermi constant. In the absence of a large lepton asymmetry, the matter mixing angle is

$$\sin^2(2\theta_m) = \frac{\sin^2(2\theta)}{\sin^2(2\theta) + \left[\cos(2\theta) - 2\epsilon T V_T/m_s^2\right]^2}\,, \tag{2.3}$$

where for ν_e the thermal potential is $V_T = -10.88 \times 10^{-9}$ GeV^{-4}.

If $f_{\nu_s} \ll f_{\nu_\alpha}$, f_{ν_s} can be neglected on the right hand side of eq. (2.1), which amounts to neglecting the inverse oscillation process $\nu_s \to \nu_\alpha$. This is a good approximation for most of the large parameter space we studied with our analytic methods, $0.01\,\text{eV} < m_s < 1\,\text{MeV}$ and $10^{-13} < \sin^2 2\theta < 1$. However, this approximation fails for very large mixing angles, for which sterile neutrinos thermalize, thus $f_{\nu_s} = f_{\nu_\alpha}$ and the right hand side of eq. (2.1) vanishes.

The "linear" equation eq. (2.1) without f_{ν_s} in the right hand side, can be analytically solved for f_{ν_s}, to obtain what we call now $f_{\nu_s-\rm lin}$ (see Paper I for a detailed discussion) for all the cosmologies we consider,

$$\begin{aligned}
f^{\rm STD}_{\nu_s-\rm lin}(\epsilon) &= 1.04 \times 10^{-5}\left(\frac{\sin^2(2\theta)}{10^{-10}}\right)\left(\frac{m_s}{\rm keV}\right)\left(\frac{g_*}{30}\right)^{-\frac{1}{2}}\left(\frac{d_\alpha}{1.27}\right) f_{\nu_\alpha}(\epsilon)\,,\\
f^{\rm K}_{\nu_s-\rm lin}(\epsilon) &= 4.2 \times 10^{-7}\epsilon^{\frac{1}{3}}\left(\frac{\sin^2(2\theta)}{10^{-10}}\right)\left(\frac{m_s}{\rm keV}\right)^{\frac{2}{3}}\left(\frac{g_*}{30}\right)^{-\frac{1}{2}}\left(\frac{d_\alpha}{1.27}\right) f_{\nu_\alpha}(\epsilon)\,,\\
f^{\rm ST1}_{\nu_s-\rm lin}(\epsilon) &= 2.2 \times 10^{-10}\epsilon^{-0.27}\left(\frac{\sin^2(2\theta)}{10^{-10}}\right)\left(\frac{m_s}{\rm keV}\right)^{1.27}\left(\frac{g_*}{30}\right)^{-\frac{1}{2}}\left(\frac{d_\alpha}{1.27}\right) f_{\nu_\alpha}(\epsilon)\,,\\
f^{\rm ST2}_{\nu_s-\rm lin}(\epsilon) &= 3.25 \times 10^{-4}\left(\frac{\sin^2(2\theta)}{10^{-10}}\right)\left(\frac{m_s}{\rm keV}\right)\left(\frac{g_*}{30}\right)^{-\frac{1}{2}}\left(\frac{d_\alpha}{1.27}\right) f_{\nu_\alpha}(\epsilon)\\
f^{\rm LRT}_{\nu_s-\rm lin} &= 3.6 \times 10^{-10}\,\epsilon\left(\frac{\sin^2(2\theta)}{10^{-10}}\right)\left(\frac{d_\alpha}{1.13}\right) f_{\nu_\alpha}(\epsilon)\,.
\end{aligned} \tag{2.4}$$

Integrating these distributions over momentum yields the corresponding "linear" number densities $n_{\nu_s-\rm lin}$. Requiring the present sterile neutrino energy density not to exceed the

JCAP10(2020)A01

present dark matter (DM) density $m_s n_{\nu_s-\mathrm{lin}}/\rho_c < \rho_{DM}/\rho_c = \Omega_{DM}$, where ρ_c is the critical density, yields the "old" mixing angle limits found in Paper I (in the linear approximation),

$$\begin{aligned}
\sin^2(2\theta)^{\mathrm{STD}}_{\mathrm{old}} &= 3.58\times10^{-7}\left(\frac{m_s}{\mathrm{keV}}\right)^{-2}\left(\frac{g_*}{30}\right)^{\frac{3}{2}}\left(\frac{d_\alpha}{1.27}\right)^{-1}\left(\frac{\Omega_{\mathrm{DM}}h^2}{0.12}\right)^{-1},\\
\sin^2(2\theta)^{\mathrm{K}}_{\mathrm{old}} &= 6.26\times10^{-6}\left(\frac{m_s}{\mathrm{keV}}\right)^{-\frac{5}{3}}\left(\frac{g_*}{30}\right)^{\frac{3}{2}}\left(\frac{d_\alpha}{1.27}\right)^{-1}\left(\frac{\Omega_{\mathrm{DM}}h^2}{0.12}\right)^{-1},\\
\sin^2(2\theta)^{\mathrm{ST1}}_{\mathrm{old}} &= 2.19\times10^{-2}\left(\frac{m_s}{\mathrm{keV}}\right)^{-2.27}\left(\frac{g_*}{30}\right)^{\frac{3}{2}}\left(\frac{d_\alpha}{1.27}\right)^{-1}\left(\frac{\Omega_{\mathrm{DM}}h^2}{0.12}\right)^{-1},\\
\sin^2(2\theta)^{\mathrm{ST2}}_{\mathrm{old}} &= 1.15\times10^{-8}\left(\frac{m_s}{\mathrm{keV}}\right)^{-2}\left(\frac{g_*}{30}\right)^{\frac{3}{2}}\left(\frac{d_\alpha}{1.27}\right)^{-1}\left(\frac{\Omega_{\mathrm{DM}}h^2}{0.12}\right)^{-1},\\
\sin^2(2\theta)^{\mathrm{LRT}}_{\mathrm{old}} &= 1\times10^{-3}\left(\frac{m_s}{\mathrm{keV}}\right)^{-1}\left(\frac{d_\alpha}{1.13}\right)^{-1}\left(\frac{\Omega_{\mathrm{DM}}h^2}{0.12}\right)^{-1}.
\end{aligned} \tag{2.5}$$

The way in which f_{ν_s} approaches f_{ν_α} with increasing mixing angle is quantified by the solution to eq. (2.1) which we call "non-linear" $f_{\nu_s-\mathrm{nl}}$ [24],

$$f_{\nu_s-\mathrm{nl}}(\epsilon,T) = \left(1-e^{-K(\epsilon,T)}\right) f_{\nu_\alpha} = \left[1-\exp\left(-\frac{f_{\nu_s-\mathrm{lin}}(\epsilon,T)}{f_{\nu_\alpha}(\epsilon)}\right)\right] f_{\nu_\alpha}(\epsilon)\,. \tag{2.6}$$

Here, $K(\epsilon,T)$ is

$$K(\epsilon,T) = \int_T^\infty dT\,\left(\frac{\Gamma_s(\epsilon,T)}{HT}\right)_\epsilon = \frac{f_{\nu_s-\mathrm{lin}}(\epsilon,T)}{f_{\nu_\alpha}(\epsilon)}\,, \tag{2.7}$$

for all the cosmologies we consider except LRT, for which the upper limit of integration is T_{RH} (see below). Notice that the integral in eq. (2.7) is performed while keeping ϵ constant. We assume that there are no sterile neutrinos present before non-resonant production takes place. Eq. (2.6) can be easily verified to be the solution to eq. (2.1) by substitution. Our previous solution is readily recovered eq. (2.6) as $f_{\nu_s-\mathrm{lin}}$ becomes much smaller than f_{ν_α} and we then keep only the first non-trivial term in the exponential.

Eq. (2.7) corresponds to eq. (3.10) of Paper I, except that in Paper I we approximated the lower limit of integration with $T=0$. This is justified as the temperatures of interest in eq. (2.6), the lower limits of integration in eq. (2.7), are much lower than the temperature T_{max} at which the sterile neutrino production rate $(\partial f_{\nu_s}/\partial T)_\epsilon$ (neglecting f_{ν_s} in the right hand side of eq. (2.1)) has a sharp maximum. For the STD cosmology, T_{max} is

$$T^{\mathrm{STD}}_{\mathrm{max}} = 145\ \mathrm{MeV}\left(\frac{m_s}{\mathrm{keV}}\right)^{\frac{1}{3}}\epsilon^{-\frac{1}{3}}\,, \tag{2.8}$$

and it is similar in the K, ST1 and ST2 cosmologies (see eqs. (3.8), (3.9), (A.2) and (A.3) of Paper I). This is a good approximation for the STD, ST1, ST2 and K cosmologies. In the LRT model, all of the sterile neutrino production is assumed to occur only during the late standard cosmology phase, at $T < T_{\mathrm{RH}}$ below the reheating temperature. Thus, the upper limit of integration in eq. (2.7) becomes T_{RH}. As the maximum of the production happens very close to T_{RH}, the lower limit of integration can again be taken to be $T=0$. This is the reason why the $f_{\nu_s-\mathrm{lin}}$ in eq. (2.4) are function of ϵ only (and not T). Therefore, from eq. (2.6) we see that $f_{\nu_s-\mathrm{nl}}$ are also functions only of ϵ.

JCAP10(2020)A01

Notice that $f_{\nu_s-\mathrm{nl}}$ in eq. (2.6) approaches the active neutrino distribution as the linear solution $f_{\nu_s-\mathrm{lin}}$ grows larger than f_{ν_α}. This $f_{\nu_s-\mathrm{lin}}$ is a non-physical solution of the Boltzmann equation due to not taking into account f_{ν_s} on the right hand side.

As we will now show, the function $f_{\nu_s-\mathrm{nl}}$ departs significantly from the linear solution $f_{\nu_s-\mathrm{lin}}$ for mixing angles that are forbidden by the DM density condition $\Omega_s < \Omega_{\mathrm{DM}}$ and by the upper limit $N_{\mathrm{eff}} < 3.4$ on the effective number of relativistic active neutrino species present during BBN. As these regions are already forbidden, the resulting limits of Paper I are unaffected by thermalization considerations.

In order to derive all limits that depend on the sterile neutrino number density n_{ν_s}, one needs to integrate $f_{\nu_s-\mathrm{nl}}$ over momenta to obtain n_{ν_s}. Following our previous notation we will denote the integration result as "non-linear" number density $n_{\nu_s-\mathrm{nl}}$, and the number densities we presented before in Paper I as "linear" $n_{\nu_s-\mathrm{lin}}$. The integration needs to be performed numerically, unless the ratio $(f_{\nu_s-\mathrm{lin}}/f_{\nu_\alpha})$ is a constant independent of ϵ. This is the case for the STD and ST2 cosmologies, where

$$\left(\frac{n_{\nu_s-\mathrm{lin}}}{n_{\nu_\alpha}}\right) = \left(\frac{f_{\nu_s-\mathrm{lin}}}{f_{\nu_\alpha}}\right) \tag{2.9}$$

and we can obtain the exact solution for $n_{\nu_s-\mathrm{nl}}$,

$$\left(\frac{n_{\nu_s-\mathrm{nl}}}{n_{\nu_\alpha}}\right) = 1 - e^{-(n_{\nu_s-\mathrm{lin}}/n_{\nu_\alpha})}\,. \tag{2.10}$$

Following our analysis of Paper I, we will proceed with an analytic treatment. We are going to find approximate analytic solutions for $n_{\nu_s-\mathrm{nl}}$ for the other cosmologies we consider in which eq. (2.9) does not hold, because the ratio $(f_{\nu_s-\mathrm{lin}}/f_{\nu_\alpha})$ depends on ϵ. The exact solution would require integration over momentum of an exponential function of ϵ. Since the dependence of the $(f_{\nu_s-\mathrm{lin}}/f_{\nu_\alpha})$ ratio on ϵ is weak, our approximation is justified.

With the DM abundance $\Omega_{\mathrm{DM}}h^2 = 0.12$, a fully thermalized sterile neutrino, with the relic number density of an active neutrino species, would constitute all of the DM if its mass is $m_s = 11.5$ eV. Thus, the DM limit $\Omega_s < \Omega_{\mathrm{DM}}$ does not restrict sterile neutrinos with $m_s < 11.5$ eV, since the number density of sterile neutrinos is at most equal to that of one active neutrino species. Above and close to $m_s = 11.5$ eV, taking into account the non-linear solution $f_{\nu_s-\mathrm{nl}}$ modifies the DM density limit with respect to the results of Paper I.

In order to find an approximate analytic solution for $n_{\nu_s-\mathrm{nl}}$, let us start by defining a pre-factor C such that eq. (A.10) of ref. [25] for the sterile neutrino relic number density is

$$n_{\nu_s-\mathrm{lin}} = C \sin^2 2\theta \tag{2.11}$$

(i.e. C includes all the factors independent of the active-sterile mixing angle). Then the non-linear solution n_{ν_s-nl} for the number density satisfies

$$\rho_{\mathrm{DM}} = \frac{m_s\, n_{\nu_s-nl}}{\Omega_s/\Omega_{\mathrm{DM}}} = 11.5 \text{ eV } n_{\nu_\alpha}\,. \tag{2.12}$$

We denoted the DM density limit obtained using $n_{\nu_s-\mathrm{lin}}$, as in Paper I, as $(\sin^2 2\theta)_{\mathrm{old}}$ that is a function of m_s given in eq. (2.5). Thus, we can now state eq. (A.25) of Paper I for the DM fraction in sterile neutrinos for the K and ST2 cosmologies (or specifically eqs. (A.26)

and (A.27) of Paper I) and eq. (A.28) of Paper I for the same fraction for the LRT model, setting these fractions to 1, as

$$1 = \frac{n_{\nu_s-\mathrm{lin}} m_s}{\rho_{\mathrm{DM}}\ (\Omega_s/\Omega_{\mathrm{DM}})} = \frac{C(\sin^2 2\theta)_{\mathrm{old}} m_s}{\rho_{\mathrm{DM}}\ (\Omega_s/\Omega_{\mathrm{DM}})}\,. \tag{2.13}$$

Using eqs. (2.11), (2.12) and (2.13) we can relate n_{ν_s-nl} with the Paper I DM limit $(\sin^2 2\theta)_{\mathrm{old}}$,

$$\frac{C(\sin^2 2\theta)_{\mathrm{old}}}{n_{\nu_\alpha}} = \frac{(\Omega_s/\Omega_{\mathrm{DM}})\ \rho_{\mathrm{DM}}}{m_s n_{\nu_\alpha}} = \frac{(\Omega_s/\Omega_{\mathrm{DM}})\ 11.5\ \mathrm{eV}}{m_s} = \frac{n_{\nu_s-nl}}{n_{\nu_\alpha}}\,. \tag{2.14}$$

This allows to define $(\sin^2 2\theta)_{\mathrm{new}}$ such that the ratio $(n_{\nu_s-\mathrm{nl}}/n_{\nu_\alpha})$ in eq. (2.10) satisfies eq. (2.14) when $(\sin^2 2\theta)_{\mathrm{new}}$ is used in $n_{\nu_s-\mathrm{lin}}$ in the exponent in the same equation, so that $(n_{\nu_s-\mathrm{nl}}/n_{\nu_\alpha}) = (\Omega_s/\Omega_{\mathrm{DM}})\ 11.5\ \mathrm{eV}/m_s$. Hence,

$$\frac{(\Omega_s/\Omega_{\mathrm{DM}})\ 11.5\ \mathrm{eV}}{m_s} = 1 - \exp\left(-\frac{C(\sin^2 2\theta)_{\mathrm{new}}}{n_{\nu_\alpha}}\right)\,. \tag{2.15}$$

Replacing here n_{ν_α} by $C(\sin^2 2\theta)_{\mathrm{old}} m_s/(\Omega_s/\Omega_{\mathrm{DM}})\ 11.5$ eV using eq. (2.14), eq. (2.15) can be rearranged to give the new mixing angle for the DM density limit (plotted in the figures) in terms of the old mixing angle (see eqs. (A.29) to (A.32) of Paper I)

$$(\sin^2 2\theta)_{\mathrm{new}} = (\sin^2 2\theta)_{\mathrm{old}}\ \frac{m_s}{(\Omega_s/\Omega_{\mathrm{DM}})\ 11.5\ \mathrm{eV}}\ \ln\left[\frac{m_s}{m_s - (\Omega_s/\Omega_{\mathrm{DM}})\ 11.5\ \mathrm{eV}}\right]\,. \tag{2.16}$$

Taking $(\Omega_s/\Omega_{\mathrm{DM}}) = 1$ this is the boundary of the dark gray regions where $\Omega_s > \Omega_{\mathrm{DM}}$ shown in figure 1 and figure 2. Except in a region close to or below $m_s = 11.5\,\mathrm{eV}$, which is rejected by the (cyan) N_{eff} BBN limit, the present DM density limits are the same as those in Paper I. Thus the allowed regions have not changed.

3 Thermalization

The production of sterile neutrinos saturates when they thermalize, when $f_{\nu_s} = f_{\nu_\alpha}$, and thus the right hand side of the Boltzmann equation eq. (2.1) is equal to zero. In figure 2, the region of thermalization where $\Gamma/H|_{T_{\mathrm{max}}} \geq 1$ is demarcated with a solid blue line at its lower boundary. When the maximum production rate $\Gamma(T_{\mathrm{max}})$ stays roughly equal to or larger than the Hubble parameter for a significant period of time, a substantial amount of sterile neutrinos are produced and the population is nearly or fully thermalized.

To compute the production rates and momentum distributions we use as the characteristic momentum $\epsilon = \langle\epsilon\rangle$. $\langle\epsilon\rangle$ is the average value of E/T for each cosmology (see eqs. (3.27) and (3.28) of Paper I)

$$\langle\epsilon\rangle = \begin{cases} 3.15, & \mathrm{STD} \\ 3.47, & \mathrm{K} \\ 2.89, & \mathrm{ST1} \\ 3.15, & \mathrm{ST2} \\ 4.11, & \mathrm{LRT} \end{cases} \tag{3.1}$$

In contrast to Paper I, except for LRT we use two values of the effective number of degrees of freedom contributing to the radiation density in H, $g_* = 10.75$ for $m_s < 11.5$ eV and $g_* = 30$ for $m_s > 11.5$ eV. This choice allows to better approximate the evolution of g_* with temperature [26–28]. We have chosen $m_s = 11.5\,\mathrm{eV}$ as the mass where g_* changes, because

JCAP10(2020)A01

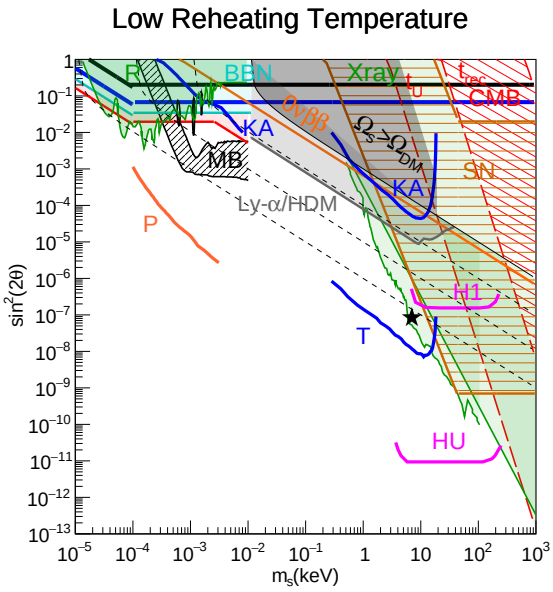

Figure 1. Present relic abundance, limits and regions of interest in the mass-mixing space of a ν_s mixed with ν_e, for the LRT cosmology with $T_{\rm RH} = 5\,{\rm MeV}$ [17]. $g_* = 10.75$ is used for $m_s < 11.5$ eV, and $g_* = 30$ above. Shown are lines of $\Omega_s/\Omega_{\rm DM} = 1$ (black solid line), 10^{-1}, 10^{-2} and 10^{-3} (black dotted lines), the forbidden region $\Omega_s/\Omega_{\rm DM} > 1$ (shaded in dark gray), lifetimes $\tau = t_U$, $t_{\rm rec}$ and $t_{\rm th}$ of Majorana ν_s (long dashed red lines), the region (SN) disfavored by supernovae [29] (horizontally hatched in brown), the location of the 3.5 keV X-ray signal [30, 31] (black star). The regions rejected by reactor neutrino (R) experiments (Daya Bay [32], Bugey-3 [33] and PROSPECT [34]) shown in green, limits on $N_{\rm eff}$ during BBN [35] (BBN) in cyan, Lyman-alpha limits [36] (Ly-α/HDM) shaded in light gray, X-ray limits [37–39] including DEBRA [40] (Xray) in green, $0\nu\beta\beta$ decays [41] ($0\nu\beta\beta$) in orange and CMB spectrum distortions [42] (CMB) diagonally hatched in red. Current/future sensitivity of KATRIN (KA) in the keV [43] and eV [44] mass range, its TRISTAN upgrade in 3 yr (T) [43] shown by blue solid lines. Magenta solid lines show the reach of the phase 1A (H1) of HUNTER, and its upgrade (HU) [45]. The 4-σ band of compatibility with LSND and MiniBooNE results (MB) in figure 4 of [46] is shown densely hatched in black. The three black vertical elliptical contours are the regions allowed at 3-σ by DANSS [47] and NEOS [48] data in figure 4 of [49]). Orange solid lines show the reach of PTOLEMY for 100 g-yr (P) exposure (from figures 6 and 7 of [50]). See Paper I for details. The thick blue line represents the thermalization condition $f_{\nu_s-{\rm lin}} = f_{\nu_\alpha}$ and the thick black line shows $f_{\nu_s-{\rm lin}} = 3 f_{\nu_\alpha}$. Notice that the LRT model goes into the standard cosmology, thus all limits become those standard, when $T_{\rm max} < T_{\rm RH} = 5\,{\rm MeV}$, i.e. for $m_s < 0.1\,{\rm eV}$. The red lines in the upper-left hand corner denotes the Planck 2018 $\Delta N_{\rm eff}$ and $m_{\rm eff}$ bounds [51].

for this mass $T_{\rm max} \simeq 20\,{\rm MeV}$ and this is the temperature above which g_* starts increasing from its value of 10.75. In Paper I we had adopted for simplicity $g_* = 30$ throughout the entire mass range, except for the $N_{\rm eff}$ BBN limit, which is particularly relevant for light sterile neutrinos, and the LRT cosmology, for which we used 10.75. Here we instead adopt $g_* = 10.75$ for all our calculations with $m_s < 11.5\,{\rm eV}$ as this value is more appropriate to the sterile neutrino production and thermalization at the eV scale, specifically in the regions where possible LSND, MiniBooNE, DANSS and NEOS sterile neutrino detection signals have been suggested. Our choice of using two distinct values of g_* results in an artificial discontinuity[1]

[1]Had we instead considered the true value of g_* that is a continuous function of temperature, such discontinuity would be absent.

JCAP10(2020)A01

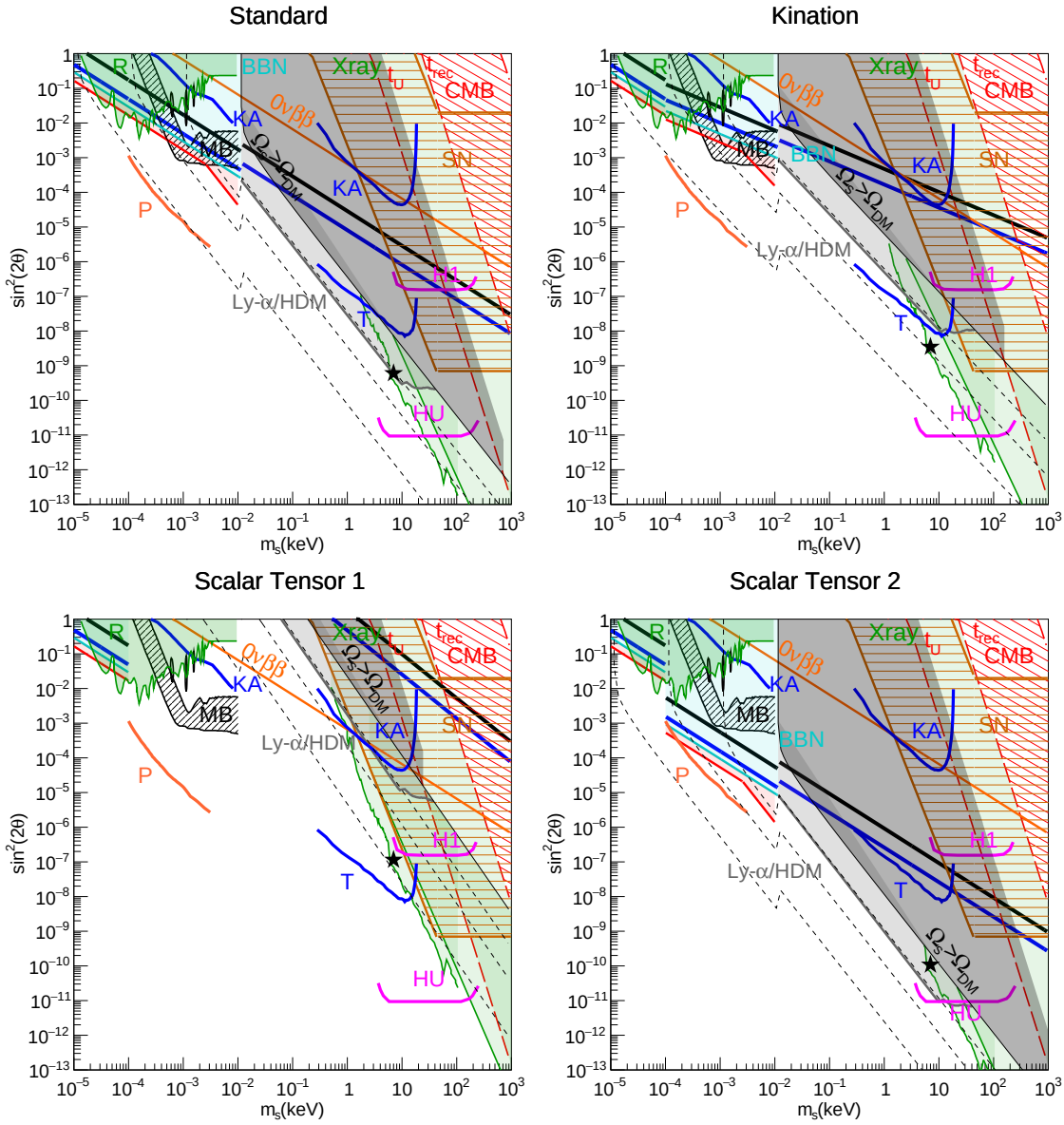

Figure 2. Present relic abundance, limits and regions of interest for standard, kination and scalar-tensor cosmologies. See figure 1 caption. Here the thick blue line represents the condition $\Gamma/H|_{T_{\max}} = 1$ that coincides with $f_{\nu_s} = f_{\nu_\alpha}$ as in figure 1. The discontinuity in the limits at $m_s = 11.5\,\text{eV}$ is due to our use of just two values for g_*, 10.75 below and 30 above (see explanations in the text). The red lines in the upper left hand corner show the Planck 2018 ΔN_{eff} and m_{eff} bounds. Notice that all cosmologies go into the standard cosmology, thus all limits become those standard, when $T_{\max} < T_{\text{tr}} = 5\,\text{MeV}$, i.e. for $m_s < 0.1\,\text{eV}$.

at $m_s = 11.5\,\text{eV}$ in all the limits in figure 2. In the LRT cosmology, production happens only at $T < 5\,\text{MeV}$, for which $g_* = 10.75$, for all sterile neutrinos. Thus there are no discontinuities at $m_s = 11.5\,\text{eV}$ in the BBN N_{eff} and thermalization (cyan, blue and black) limits in figure 1.

Notice that all cosmologies go into the standard cosmology, thus all limits become those standard, when $T_{\max} < T_{\text{tr}} = 5\,\text{MeV}$, i.e. for $m_s < 0.1\,\text{eV}$. Given our approximations of considering a sharp transition of all cosmologies into the standard one at T_{tr}, and assuming

JCAP10(2020)A01

the sterile neutrino production happens at $T_{\rm max}$, this results in a discontinuity at $m_s \simeq 0.1$ eV in the limits in figure 1 and 2, which had not been included in Paper I (as it affects a very small portion of the whole mass range we considered). In a more careful treatment, the limits would smoothly transition from the non-standard to the standard ones.

Solving for $\sin^2 2\theta$ from the condition $\Gamma/H|_{T_{\rm max}} = 1$ we obtain the following thermalization limits (the solid thick blue lines in figure 2),

$$\text{for STD:} \qquad (\sin^2 2\theta)_{\rm th} = 4.86 \times 10^{-3} \left(\frac{d_\alpha}{1.27}\right)^{-1} \left(\frac{m_s}{\rm eV}\right)^{-1} \left(\frac{g_*}{10.75}\right)^{\frac{1}{2}} , \tag{3.2}$$

$$\text{for K:} \qquad (\sin^2 2\theta)_{\rm th} = 1.52 \times 10^{-2} \epsilon^{-\frac{1}{3}} \left(\frac{d_\alpha}{1.27}\right)^{-1} \left(\frac{m_s}{\rm eV}\right)^{-\frac{2}{3}} \left(\frac{g_*}{10.75}\right)^{\frac{1}{2}} , \tag{3.3}$$

$$\text{for ST1:} \qquad (\sin^2 2\theta)_{\rm th} = 1.38 \times 10^{3} \epsilon^{0.27} \left(\frac{d_\alpha}{1.27}\right)^{-1} \left(\frac{m_s}{\rm eV}\right)^{-1.27} \left(\frac{g_*}{10.75}\right)^{\frac{1}{2}} , \tag{3.4}$$

$$\text{and for ST2:} \qquad (\sin^2 2\theta)_{\rm th} = 1.56 \times 10^{-4} \left(\frac{d_\alpha}{1.27}\right)^{-1} \left(\frac{m_s}{\rm eV}\right)^{-1} \left(\frac{g_*}{10.75}\right)^{\frac{1}{2}} . \tag{3.5}$$

We have confirmed that these limits (derived from $\Gamma/H|_{T_{\rm max}} = 1$) practically coincide with those corresponding to $f_{\nu_s-{\rm lin}} = f_{\nu_\alpha}$ for the mentioned cosmologies, which we thus do not display separately in figure 2.

For the LRT model, considering that the maximum production rate is at $T_{\rm RH} = 5\,{\rm MeV}$, we could be tempted to use $\Gamma/H|_{T_{\rm RH}} = 1$ as the condition for thermalization. However, when employing this condition throughout the whole range of integration in T, from 0 to $T_{\rm RH}$, to obtain $K(\epsilon, T)$, the integrand is smaller than 1. Thus, this is not a good condition of thermalization for this model. Since the thermalization condition based on Γ/H coincides with the condition $f_{\nu_s-{\rm lin}} = f_{\nu_\alpha}$ in all the other models we consider, we thus adopt $f_{\nu_s-{\rm lin}} = f_{\nu_\alpha}$ as the condition for thermalization in the LRT model. This condition translates into

$$(\sin^2 2\theta)_{\rm th} = 2.78 \times 10^{-1}\ \epsilon^{-1} , \tag{3.6}$$

which is shown with the thick blue line in figure 1.

Notice that we have considered the condition $\Gamma/H > 1$ for chemical equilibrium of sterile neutrinos, since the rate Γ we used is the production rate. Kinetic equilibrium happens at larger mixing angles than chemical equilibrium. The reason for this is that the sterile neutrino scattering rate contains an extra $\sin^2\theta$ factor over the production rate. Thus, sterile neutrinos that are not in chemical equilibrium (i.e. for which the production rate is $\Gamma < H$) are also not in kinetic equilibrium, they are decoupled from the thermal bath.

On the thick blue lines in the figures, $f_{\nu_s-{\rm nl}} = (1 - e^{-1}) f_{\nu_\alpha} = 0.63 f_{\nu_\alpha}$. In figure 1 and figure 2 we also display with a solid black line where $f_{\nu_s-{\rm lin}} = 3 f_{\nu_\alpha}$, and thus $f_{\nu_s-{\rm nl}} = (1 - e^{-3}) f_{\nu_\alpha} = 0.95 f_{\nu_\alpha}$, where nearly full thermalization occurs. Above this black line, the sterile neutrino momentum distribution rapidly becomes $f_{\nu_s} = f_{\nu_\alpha}$ with increased mixing (i.e. the right hand side of the Boltzmann equation eq. (2.1) goes to zero). The equations of the thick black line in the figures are:

$$\text{for STD:} \qquad \sin^2 2\theta = 1.73 \times 10^{-2} \left(\frac{d_\alpha}{1.27}\right)^{-1} \left(\frac{m_s}{\rm eV}\right)^{-1} \left(\frac{g_*}{10.75}\right)^{\frac{1}{2}} , \tag{3.7}$$

$$\text{for K:} \qquad \sin^2 2\theta = 4.29 \times 10^{-2} \epsilon^{-\frac{1}{3}} \left(\frac{d_\alpha}{1.27}\right)^{-1} \left(\frac{m_s}{\rm eV}\right)^{-\frac{2}{3}} \left(\frac{g_*}{10.75}\right)^{\frac{1}{2}} , \tag{3.8}$$

JCAP10(2020)A01

$$\text{for ST1:} \qquad \sin^2 2\theta = 5.27 \times 10^3 \epsilon^{0.27} \left(\frac{d_\alpha}{1.27}\right)^{-1} \left(\frac{m_s}{\text{eV}}\right)^{-1.27} \left(\frac{g_*}{10.75}\right)^{\frac{1}{2}} , \tag{3.9}$$

$$\text{for ST2:} \qquad \sin^2 2\theta = 5.52 \times 10^{-4} \left(\frac{d_\alpha}{1.27}\right)^{-1} \left(\frac{m_s}{\text{eV}}\right)^{-1} \left(\frac{g_*}{10.75}\right)^{\frac{1}{2}} , \tag{3.10}$$

$$\text{and for LRT:} \qquad \sin^2 2\theta = 8.34 \times 10^{-1} \epsilon^{-1} . \tag{3.11}$$

Eqs. (2.9) and (2.10) emply that $f_{\nu_s-\text{lin}} = 3 f_{\nu_\alpha}$ corresponds to $n_{\nu_s-\text{nl}}/n_{\nu_\alpha} \simeq 0.95$, which leads to $\rho_s = \rho_{\text{DM}}$ for $m_s = 11.5\,\text{eV}$. In fact, in the figures the thick blue line intersects the DM density limit near $m_s = 11.5\,\text{eV}$, as expected.

4 Bounds

We include here the same bounds detailed in Paper I with a few modifications. As we explain below, due to solving for the non-linear number densities as described in the preceding sections, both the BBN ΔN_{eff} and Ly-α bounds move here to larger mixings with respect to those in Paper I, and also add here the CMB ΔN_{eff} and m_{eff} bounds [51], which we had neglected in Paper I because they are very close to the BBN ΔN_{eff} limit).

To derive the Lyman-α bound we used the 2-σ warm DM limit from SDSS+XQ+HR in figure 6 of ref. [36], which has an asymptote of $(\Omega_s/\Omega_{\text{DM}}) \lesssim 0.08$ for small sterile neutrino masses. This limit is given in terms of m_{therm} which can be converted to limits on m_s using [52] $m_s = 4.46\ \text{keV}\,(\langle\epsilon\rangle/3.15)\,(m_{\text{therm}}/\text{keV})^{\frac{4}{3}}\,(T_{\nu_s}/T_{\nu_\alpha})\,\big(0.12/(\Omega_s\ h^2)\big)^{\frac{1}{3}}$. We apply eq. (2.16) with $(\Omega_s/\Omega_{\text{DM}}) = 0.08$ replacing $(\sin^2 2\theta)_{\text{old}}$ by the Lyman-α limits in Paper I, to obtain the present Lyman-α bounds. The Lyman-α limits are shown up to their intersection with THE BBN N_{eff} bounds. Using eq. (2.10) we obtain the BBN $\Delta N_{\text{eff}} \leq 0.4$ [35] limit, which translates into $n_{\nu_s-\text{lin}}/n_{\nu_a} \leq 0.51$.

We apply for $m_s \lesssim 10$ eV the combined CMB ΔN_{eff} and m_{eff} [51], for sterile neutrinos which are respectively relativistic and becoming non-relativistic close recombination. The current 95% Planck 2018 limits in eq. (70a) of ref. [51] are[2]

$$N_{\text{eff}} < 3.29, \qquad m_{\text{eff}} < 0.65\ \text{eV} . \tag{4.1}$$

Using the definitions $N_{\text{eff}} = 3.04 + (\rho_{\nu_s}/\rho_{\nu_\alpha})$ and $m_{\text{eff}} = n_{\nu_s} m_s/n_{\nu_a}$ [24, 51] with $\rho_{\nu_s}/\rho_{\nu_\alpha} = (\langle\epsilon\rangle\ n_{\nu_s-\text{nl}})/(3.15\ n_{\nu_a})$ and $n_{\nu_s} = n_{\nu_s-\text{nl}}$, and replacing in eq. (2.10) the upper limits on $n_{\nu_s-\text{nl}}$ derived from the N_{eff} and the m_{eff} limits we get respectively

$$\frac{n_{\nu_s-\text{lin}}}{n_{\nu_\alpha}} < \ln\left(\frac{1}{1-0.25(3.15/\langle\epsilon\rangle)}\right) \simeq 0.29, \qquad \frac{n_{\nu_s-\text{lin}}}{n_{\nu_a}} < -\ln\left[1-\frac{0.65\ \text{eV}}{m_s}\right] . \tag{4.2}$$

Using now eqs. (3.18), (3.20), (A.12), (A.14), and (A.16) of Paper I for $n_{\nu_s-\text{lin}}$, we obtain the upper limits on the mixing angle shown with red solid lines in the upper left hand corners of figures 1 and 2 for $m_s < 10$ eV. The m_{eff} bound becomes more restrictive than the ΔN_{eff} bound for $m_s > 3$ eV, which causes the change in slope of the red lines. As it is clear from the figures, these CMB limits are very close to the BBN N_{eff} (cyan) limits, thus do not change significantly the allowed parameter regions (as we argued in Paper I to neglect them).

[2] While these bounds were formulated for thermally produced sterile neutrinos, they are expected to be reasonably accurate for other models [53]. We thus apply them to all cosmologies.

JCAP10(2020)A01

5 Concluding remarks

We have considered the approach of sterile neutrinos to thermalization that happens for large enough active-sterile mixing angles. We showed that the allowed regions of parameter space found in Paper I are not affected by these considerations. In particular, the interesting region in which there are several suggested potential signals of a light sterile neutrino with mass close to 1 eV are free from cosmological bounds in the ST1 and LRT cosmologies.

Acknowledgments

The work of G.B.G., P.L. and V.T. was supported in part by the U.S. Department of Energy (DOE) Grant No. DE-SC0009937.

References

[1] G.B. Gelmini, P. Lu and V. Takhistov, *Cosmological Dependence of Non-resonantly Produced Sterile Neutrinos*, *JCAP* **12** (2019) 047 [arXiv:1909.13328] [INSPIRE].

[2] G.B. Gelmini, P. Lu and V. Takhistov, *Visible Sterile Neutrinos as the Earliest Relic Probes of Cosmology*, *Phys. Lett. B* **800** (2020) 135113 [arXiv:1909.04168] [INSPIRE].

[3] T. Hasegawa, N. Hiroshima, K. Kohri, R.S.L. Hansen, T. Tram and S. Hannestad, *MeV-scale reheating temperature and cosmological production of light sterile neutrinos*, *JCAP* **08** (2020) 015 [arXiv:2003.13302] [INSPIRE].

[4] T. Hasegawa, N. Hiroshima, K. Kohri, R.S.L. Hansen, T. Tram and S. Hannestad, *MeV-scale reheating temperature and thermalization of oscillating neutrinos by radiative and hadronic decays of massive particles*, *JCAP* **12** (2019) 012 [arXiv:1908.10189] [INSPIRE].

[5] P.F. de Salas, M. Lattanzi, G. Mangano, G. Miele, S. Pastor and O. Pisanti, *Bounds on very low reheating scenarios after Planck*, *Phys. Rev. D* **92** (2015) 123534 [arXiv:1511.00672] [INSPIRE].

[6] F. De Bernardis, L. Pagano and A. Melchiorri, *New constraints on the reheating temperature of the universe after WMAP-5*, *Astropart. Phys.* **30** (2008) 192 [INSPIRE].

[7] S. Hannestad, *What is the lowest possible reheating temperature?*, *Phys. Rev. D* **70** (2004) 043506 [astro-ph/0403291] [INSPIRE].

[8] M. Kawasaki, K. Kohri and N. Sugiyama, *MeV scale reheating temperature and thermalization of neutrino background*, *Phys. Rev. D* **62** (2000) 023506 [astro-ph/0002127] [INSPIRE].

[9] M. Kawasaki, K. Kohri and N. Sugiyama, *Cosmological constraints on late time entropy production*, *Phys. Rev. Lett.* **82** (1999) 4168 [astro-ph/9811437] [INSPIRE].

[10] R. Catena, N. Fornengo, A. Masiero, M. Pietroni and F. Rosati, *Dark matter relic abundance and scalar-tensor dark energy*, *Phys. Rev. D* **70** (2004) 063519 [astro-ph/0403614] [INSPIRE].

[11] R. Catena, N. Fornengo, A. Masiero, M. Pietroni and M. Schelke, *Enlarging mSUGRA parameter space by decreasing pre-BBN Hubble rate in Scalar-Tensor Cosmologies*, *JHEP* **10** (2008) 003 [arXiv:0712.3173] [INSPIRE].

[12] B. Spokoiny, *Deflationary universe scenario*, *Phys. Lett. B* **315** (1993) 40 [gr-qc/9306008] [INSPIRE].

[13] M. Joyce, *Electroweak Baryogenesis and the Expansion Rate of the Universe*, *Phys. Rev. D* **55** (1997) 1875 [hep-ph/9606223] [INSPIRE].

[14] P. Salati, *Quintessence and the relic density of neutralinos*, *Phys. Lett. B* **571** (2003) 121 [astro-ph/0207396] [INSPIRE].

JCAP10(2020)A01

[15] S. Profumo and P. Ullio, *SUSY dark matter and quintessence*, *JCAP* **11** (2003) 006 [hep-ph/0309220] [INSPIRE].

[16] C. Pallis, *Quintessential kination and cold dark matter abundance*, *JCAP* **10** (2005) 015 [hep-ph/0503080] [INSPIRE].

[17] G. Gelmini, S. Palomares-Ruiz and S. Pascoli, *Low reheating temperature and the visible sterile neutrino*, *Phys. Rev. Lett.* **93** (2004) 081302 [astro-ph/0403323] [INSPIRE].

[18] G.B. Gelmini and P. Gondolo, *Neutralino with the right cold dark matter abundance in (almost) any supersymmetric model*, *Phys. Rev. D* **74** (2006) 023510 [hep-ph/0602230] [INSPIRE].

[19] G. Gelmini, P. Gondolo, A. Soldatenko and C.E. Yaguna, *The effect of a late decaying scalar on the neutralino relic density*, *Phys. Rev. D* **74** (2006) 083514 [hep-ph/0605016] [INSPIRE].

[20] G. Gelmini, E. Osoba, S. Palomares-Ruiz and S. Pascoli, *MeV sterile neutrinos in low reheating temperature cosmological scenarios*, *JCAP* **10** (2008) 029 [arXiv:0803.2735] [INSPIRE].

[21] C.E. Yaguna, *Sterile neutrino production in models with low reheating temperatures*, *JHEP* **06** (2007) 002 [arXiv:0706.0178] [INSPIRE].

[22] K.N. Abazajian, *Sterile neutrinos in cosmology*, *Phys. Rept.* **711-712** (2017) 1 [arXiv:1705.01837] [INSPIRE].

[23] S. Hannestad, I. Tamborra and T. Tram, *Thermalisation of light sterile neutrinos in the early universe*, *JCAP* **07** (2012) 025 [arXiv:1204.5861] [INSPIRE].

[24] T. Rehagen and G.B. Gelmini, *Effects of kination and scalar-tensor cosmologies on sterile neutrinos*, *JCAP* **06** (2014) 044 [arXiv:1402.0607] [INSPIRE].

[25] G.B. Gelmini, P. Lu and V. Takhistov, *Cosmological Dependence of Resonantly Produced Sterile Neutrinos*, *JCAP* **06** (2020) 008 [arXiv:1911.03398] [INSPIRE].

[26] L. Husdal, *On Effective Degrees of Freedom in the Early Universe*, *Galaxies* **4** (2016) 78 [arXiv:1609.04979] [INSPIRE].

[27] S. Borsányi et al., *Calculation of the axion mass based on high-temperature lattice quantum chromodynamics*, *Nature* **539** (2016) 69 [arXiv:1606.07494] [INSPIRE].

[28] M. Drees, F. Hajkarim and E.R. Schmitz, *The Effects of QCD Equation of State on the Relic Density of WIMP Dark Matter*, *JCAP* **06** (2015) 025 [arXiv:1503.03513] [INSPIRE].

[29] K. Kainulainen, J. Maalampi and J.T. Peltoniemi, *Inert neutrinos in supernovae*, *Nucl. Phys. B* **358** (1991) 435 [INSPIRE].

[30] E. Bulbul, M. Markevitch, A. Foster, R.K. Smith, M. Loewenstein and S.W. Randall, *Detection of An Unidentified Emission Line in the Stacked X-ray spectrum of Galaxy Clusters*, *Astrophys. J.* **789** (2014) 13 [arXiv:1402.2301] [INSPIRE].

[31] A. Boyarsky, O. Ruchayskiy, D. Iakubovskyi and J. Franse, *Unidentified Line in X-Ray Spectra of the Andromeda Galaxy and Perseus Galaxy Cluster*, *Phys. Rev. Lett.* **113** (2014) 251301 [arXiv:1402.4119] [INSPIRE].

[32] Daya Bay collaboration, *Improved Search for a Light Sterile Neutrino with the Full Configuration of the Daya Bay Experiment*, *Phys. Rev. Lett.* **117** (2016) 151802 [arXiv:1607.01174] [INSPIRE].

[33] Y. Declais et al., *Search for neutrino oscillations at 15-meters, 40-meters, and 95-meters from a nuclear power reactor at Bugey*, *Nucl. Phys. B* **434** (1995) 503 [INSPIRE].

[34] PROSPECT collaboration, *First search for short-baseline neutrino oscillations at HFIR with PROSPECT*, *Phys. Rev. Lett.* **121** (2018) 251802 [arXiv:1806.02784] [INSPIRE].

[35] Particle Data Group collaboration, *Review of Particle Physics*, *Phys. Rev. D* **98** (2018) 030001 [INSPIRE].

JCAP10(2020)A01

[36] J. Baur et al., *Constraints from Ly-α forests on non-thermal dark matter including resonantly-produced sterile neutrinos*, *JCAP* **12** (2017) 013 [arXiv:1706.03118] [INSPIRE].

[37] K.C.Y. Ng et al., *New Constraints on Sterile Neutrino Dark Matter from NuSTAR M31 Observations*, *Phys. Rev. D* **99** (2019) 083005 [arXiv:1901.01262] [INSPIRE].

[38] K. Perez, K.C.Y. Ng, J.F. Beacom, C. Hersh, S. Horiuchi and R. Krivonos, *Almost closing the νMSM sterile neutrino dark matter window with NuSTAR*, *Phys. Rev. D* **95** (2017) 123002 [arXiv:1609.00667] [INSPIRE].

[39] A. Neronov, D. Malyshev and D. Eckert, *Decaying dark matter search with NuSTAR deep sky observations*, *Phys. Rev. D* **94** (2016) 123504 [arXiv:1607.07328] [INSPIRE].

[40] A. Boyarsky, A. Neronov, O. Ruchayskiy and M. Shaposhnikov, *Constraints on sterile neutrino as a dark matter candidate from the diffuse x-ray background*, *Mon. Not. Roy. Astron. Soc.* **370** (2006) 213 [astro-ph/0512509] [INSPIRE].

[41] KamLAND-Zen collaboration, *Search for Majorana Neutrinos near the Inverted Mass Hierarchy Region with KamLAND-Zen*, *Phys. Rev. Lett.* **117** (2016) 082503 [*Addendum ibid.* **117** (2016) 109903] [arXiv:1605.02889] [INSPIRE].

[42] D.J. Fixsen, E.S. Cheng, J.M. Gales, J.C. Mather, R.A. Shafer and E.L. Wright, *The Cosmic Microwave Background spectrum from the full COBE FIRAS data set*, *Astrophys. J.* **473** (1996) 576 [astro-ph/9605054] [INSPIRE].

[43] KATRIN collaboration, *A novel detector system for KATRIN to search for keV-scale sterile neutrinos*, *J. Phys. G* **46** (2019) 065203 [arXiv:1810.06711] [INSPIRE].

[44] F. Megas, *eV-scale Sterile Neutrino Investigation with the First Tritium KATRIN Data*, MSc Thesis, Technische Universität München, Munich, Germany (2019).

[45] P.F. Smith, *Proposed experiments to detect keV range sterile neutrinos using energy-momentum reconstruction of beta decay or K-capture events*, *New J. Phys.* **21** (2019) 053022 [arXiv:1607.06876] [INSPIRE].

[46] MiniBooNE collaboration, *Significant Excess of ElectronLike Events in the MiniBooNE Short-Baseline Neutrino Experiment*, *Phys. Rev. Lett.* **121** (2018) 221801 [arXiv:1805.12028] [INSPIRE].

[47] DANSS collaboration, *Search for sterile neutrinos at the DANSS experiment*, *Phys. Lett. B* **787** (2018) 56 [arXiv:1804.04046] [INSPIRE].

[48] NEOS collaboration, *Sterile Neutrino Search at the NEOS Experiment*, *Phys. Rev. Lett.* **118** (2017) 121802 [arXiv:1610.05134] [INSPIRE].

[49] S. Gariazzo, C. Giunti, M. Laveder and Y.F. Li, *Model-independent $\bar{\nu}_e$ short-baseline oscillations from reactor spectral ratios*, *Phys. Lett. B* **782** (2018) 13 [arXiv:1801.06467] [INSPIRE].

[50] PTOLEMY collaboration, *Neutrino physics with the PTOLEMY project: active neutrino properties and the light sterile case*, *JCAP* **07** (2019) 047 [arXiv:1902.05508] [INSPIRE].

[51] Planck collaboration, *Planck 2018 results. VI. Cosmological parameters*, *Astron. Astrophys.* **641** (2020) A6 [arXiv:1807.06209] [INSPIRE].

[52] M. Viel, J. Lesgourgues, M.G. Haehnelt, S. Matarrese and A. Riotto, *Constraining warm dark matter candidates including sterile neutrinos and light gravitinos with WMAP and the Lyman-alpha forest*, *Phys. Rev. D* **71** (2005) 063534 [astro-ph/0501562] [INSPIRE].

[53] Planck collaboration, *Planck 2015 results. XIII. Cosmological parameters*, *Astron. Astrophys.* **594** (2016) A13 [arXiv:1502.01589] [INSPIRE].

JCAP10(2020)A01